



CHORUS

This is the accepted manuscript made available via CHORUS. The article has been published as:

Colloidal Adsorption at Fluid Interfaces: Regime Crossover from Fast Relaxation to Physical Aging

Carlos E. Colosqui, Jeffrey F. Morris, and Joel Koplik

Phys. Rev. Lett. **111**, 028302 — Published 9 July 2013

DOI: [10.1103/PhysRevLett.111.028302](https://doi.org/10.1103/PhysRevLett.111.028302)

Colloidal Adsorption at Fluid Interfaces: Regime Crossover from Fast Relaxation to Physical Aging.

Carlos E. Colosqui,^{1,*} Jeffrey F. Morris,[†] and Joel Koplik[‡]

¹*Benjamin Levich Institute, City College of the City University of New York, New York, NY 10031, USA*

The adsorption of a colloidal particle at a fluid interface is studied theoretically and numerically, documenting distinctly different relaxation regimes. The adsorption of a perfectly smooth particle is characterized by a fast exponential relaxation to thermodynamic equilibrium where the interfacial free energy reaches the global minimum. The short relaxation time is given by the ratio of viscous damping to capillary forces. Physical and/or chemical heterogeneities, however, can result in multiple minima of the free energy giving rise to metastability. In the presence of metastable states we observe a crossover to a slow logarithmic relaxation reminiscent of physical aging in glassy systems; sufficiently close to equilibrium the slow relaxation becomes exponential. The long relaxation time is determined by the Kramers escape rate from metastable states. Derived analytical expressions yield quantitative agreement with molecular dynamics simulations and recent experimental observations. This work provides new insights on the adsorption of colloidal particles with surface microstructure.

PACS numbers: 47.85.-g; 82.70.Dd; 47.61.Jd

The adsorption and binding of colloidal particles to fluid interfaces is relevant to numerous natural and industrial processes. Novel technological applications in areas that range from materials science to renewable energy [1, 2], and from food science to biomedicine [3, 4] demand advancements in the fundamental understanding of colloidal adsorption. Standard models based on continuum thermodynamics [1, 5] predict monotonic relaxation to an equilibrium position where the contact angle with the interface is given by Young's law [6]. This equilibrium position corresponds to a stable state determined by the (global) minimum of the Helmholtz free energy. For nano/micrometer-size particles, the energy decrease at the equilibrium state can be orders of magnitude larger than the thermal energy, and thus strong interfacial forces are expected to cause a spontaneous adsorption with rapid relaxation to equilibrium.

Nevertheless, colloidal adsorption remains poorly understood for systems of great practical interest (e.g., functionalized particles). Fundamental issues arise when the equilibrium contact angle is undeterminable, e.g., in the presence of surface heterogeneities and contact angle hysteresis [6, 7]. Even when equilibrium contact angles can be determined, it is frequently observed that colloidal adsorption is neither fast nor spontaneous and requires some form of external actuation (mechanical/thermal/chemical) to be initiated [8–10]. Notably, recent experimental work [10] reported a slow logarithmic relaxation to equilibrium after initiating the adsorption of a micrometer-size particle at a water-oil interface. The unexpected observation was attributed to nanoscale surface heterogeneities [10] and data were fitted with a dynamic wetting model due to Blake and Haynes [11].

A logarithmic relaxation is reminiscent of physical aging in glassy systems having complex energy landscapes and metastability [12]. These phenomena suggest that energy barriers associated with microscale hetero-

geneities should be considered in order to describe the slow (quasi-static) relaxation of colloidal particles at fluid interfaces. In this Letter, we study the entire dynamics of adsorption in the presence of metastable states caused by local minima of the interfacial free energy. We propose a model based on Kramers' escape from metastable states [13, 14], that quantitatively describes recent experimental observations [10]. Derived expressions and numerical simulations document different crossovers between exponential and logarithmic relaxations.

Our analysis begins with the equation of motion for a colloidal particle that straddles the interface between two immiscible fluids [cf. Fig. 1(a)]. Assuming the particle undergoes Brownian motion, its vertical position z is governed by a Langevin equation

$$m\ddot{z} = \sqrt{2k_B T \xi} \eta(t) - \xi \dot{z} + F(z); \quad (1)$$

here m is the particle mass, $k_B T$ is the thermal energy of the surrounding fluids, $\eta(t)$ is a zero-mean unit-variance Gaussian noise, ξ is the viscous friction coefficient, and $F(z) = -\partial U/\partial z$ is the interfacial or *capillary* force determined by the interfacial free energy U . In the framework of continuum thermodynamics, the energy to form an interface is the product of the interfacial area and corresponding surface tension; γ for the fluid-fluid interface, γ_{p1} and γ_{p2} for the interfaces between the particle and each fluid. Hence, for a spherical particle of radius R with its center at z and a sharp and flat fluid interface at $z = 0$, the interfacial free energy can be cast as [5]

$$U_S(z) = \frac{1}{2}K(z - z_E)^2 - C \quad \text{for } |z| \leq R, \quad (2)$$

where z_E is the equilibrium position, while $K = 2\pi\gamma$ and $C = \pi\gamma(R - z_E)^2$ are positive constants. According to Eq. 2 the interfacial force is linear, $F = -K(z - z_E)$. Employing this linear force and neglecting small inertial effects, the solution of Eq. 1 gives an average displacement

$\langle z \rangle = z_E + \Delta z \exp(-t/T_D)$, where $\Delta z = z(0) - z_E$ is the distance from equilibrium at $t = 0$ and $T_D = \xi/K$ is the viscous decay time. For reference, we note that the decay time is $T_D \sim 0.1\mu\text{s}$ for a one-micron radius particle adsorbed at a water-oil interface. Thus, the standard model predicts a fast exponential relaxation to equilibrium for a perfectly smooth particle.

A few comments are in order. For the idealized case of a perfectly smooth and spherical particle that straddles a flat interface, there is a one-to-one correspondence between the particle position z and the observed contact angle $\theta = \text{acos}(-z/R)$ which is constant along the perfectly circular contact line. According to Young's law for the equilibrium contact angle, $\cos\theta_E = (\gamma_{p2} - \gamma_{p1})/\gamma$, the particle will straddle the two fluids at an equilibrium position $z_E = -R \cos\theta_E$ when $|\gamma_{p2} - \gamma_{p1}| < \gamma$. Both Young's law and Eq. 2 for $U_S(z)$ apply to homogeneous and regular contact lines. To model surface heterogeneities and irregular contact lines, we will neglect the line tension term used in alternative models [15, 16] and consider a free energy with multiple local minima.

We are interested in a simple analytical description of microscale surface heterogeneities, as illustrated in Fig. 1(b), that can give rise to significant energy barriers $\Delta U > k_B T$. For this purpose, we introduce perturbations in the interfacial free energy of the form $\frac{1}{2}\Delta U \sin(\lambda\theta + \phi)$; here $\frac{1}{2}\Delta U$ is the amplitude of the perturbation, $l = 2\pi/\lambda$ is its wavelength, and ϕ is a variable phase, here chosen so that $U(z_E)$ is the minimum. For the sake of analytical tractability we will consider a single-mode perturbation of small wavelength, $l \ll R$, equilibrium contact angles near neutral wetting, $70^\circ \lesssim \theta_E \lesssim 110^\circ$, and conditions where the particle center is close to the fluid interface, $|z/R| \ll 1$. Curvature effects, of order $\mathcal{O}((z/R)^2)$, can thus be neglected and the interfacial free energy is expressed as

$$U(z) = U_S(z) + \frac{1}{2}\Delta U \sin(\lambda z + \phi) \quad (3)$$

while the capillary force on the particle is

$$F(z) = -K(z - z_E) - \frac{1}{2}\lambda\Delta U \cos(\lambda z + \phi). \quad (4)$$

A simplified system with dynamics governed by Eq. 1 and free energy given by Eq. 3 is depicted in Fig. 1(c). The simplified system consists of a solid surface element with sinusoidal roughness (wavelength l , height h , and width w) that straddles the fluid interface, and thus produces spatial oscillations of amplitude $\Delta U = \gamma h w$ in the interfacial free energy. Just as if the surface element formed part of a much larger spherical particle, a linear force drives the system toward equilibrium at $z = z_E$; this force corresponds to the free energy contribution U_S in Eq. 2 caused by macroscale curvature. The decomposition of macroscale and microscale features makes the problem tractable via molecular dynamics (MD) [17]. Simulated trajectories $z(t)$ from individual MD realizations shown in Fig. 1(d) exhibit metastable states with a

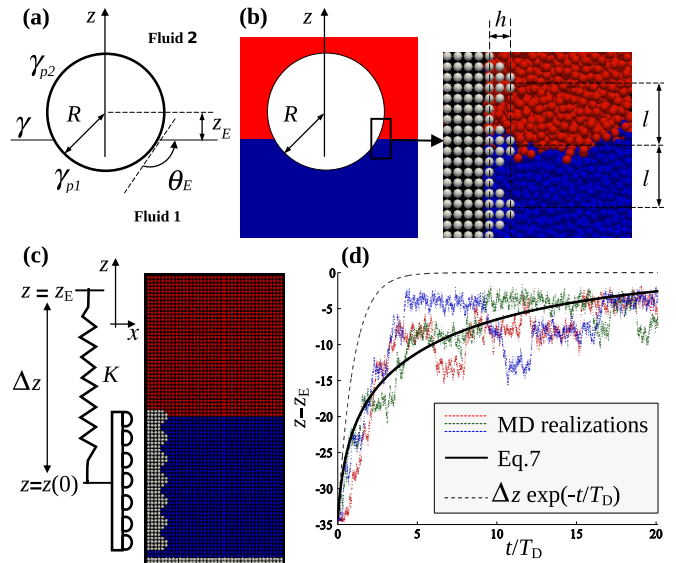


FIG. 1. Problem description and modeled system. (a) Colloidal particle of radius R straddling a sharp fluid interface. (b) Particle with microscale heterogeneities of size $l \ll R$. A surface roughness of wavelength l , height h , and width $w \sim h$ induces interfacial energy perturbations of amplitude $\Delta U = \gamma h w$. The system free energy is thus given by Eq. 3. (c) Simplified system for MD simulations with free energy given by Eq. 3. A linear “spring” force $F = K\Delta z$ drives the relaxation to equilibrium at $z = z_E$. (d) Trajectories $z(t)$ from MD simulations (dotted lines) for different realizations ($L_H = Kl/2k_B T = 7.4$, $\Delta U/k_B T = 4$, and $\Delta z = -4.5L_H$). Analytical expressions are plotted for comparison (see legend).

lifetime that increases as the equilibrium position z_E is approached.

According to Eqs. 3–4 there are multiple minima in the free energy for $|z - z_E| < \pi\Delta U/Kl$, and sufficiently close to equilibrium the system must exhibit metastability. The basins of attraction of each metastable state are centered at the local minima $z_o = z_E + l(n - \frac{1}{4} - \phi/2\pi) + \mathcal{O}(\epsilon)$ and each basin is bounded by two neighboring maxima at $z_{\pm} = z_o \pm \frac{1}{2}l + \mathcal{O}(\epsilon)$; here n is any integer and $\epsilon = Kl|z - z_E|/\pi\Delta U$ is a small parameter. A Brownian particle (see Fig. 1(d)) will transition, or “hop” back and forth, between metastable states at a local rate [13]

$$\Gamma_{\pm}(z) = \frac{1}{2\pi\xi} \sqrt{\left. \frac{\partial^2 U(z_o)}{\partial z^2} \right| \left. \frac{\partial^2 U(z_{\pm})}{\partial z^2} \right|} \exp\left(-\frac{\Delta U_{\pm}}{k_B T}\right) \quad (5)$$

predicted for $|z - z_o| < \frac{1}{2}l$. The energy barriers, $\Delta U_{\pm} = U(z_{\pm}) - U(z_o)$, in the forward/backward direction determine the Arrhenius exponential factor. The prefactor employed in Eq. 5 is valid for overdamped systems [13, 14] where $\xi > \sqrt{m|\partial^2 U(z_{\pm})/\partial z^2|}$ (here m is the particle mass). For $|z - z_E| \ll \pi\Delta U/Kl$ the motion is dominated by thermally-activated hopping, and the ensemble-averaged speed $\langle \dot{z} \rangle$ of the particle is deter-

mined by an ordinary differential equation

$$\langle \dot{z} \rangle = \frac{1}{2}l(\Gamma_+ - \Gamma_-). \quad (6)$$

A similar mathematical expression, proposed in [11] for contact line dynamics and involving adjustable parameters, has been solved in [10] to describe logarithmic behavior, albeit neglecting backward hopping ($\Gamma_- = 0$). We solve the full equation of motion, Eq. 6 derived via Kramers' theory, to obtain the average particle trajectory

$$\langle z \rangle = z_E + L_H \log \left[\frac{1 + A_H \exp(-t/T_H)}{1 - A_H \exp(-t/T_H)} \right], \quad (7)$$

which depends on three independent parameters prescribed by physical variables; i.e., the characteristic hop length $L_H = 2k_B T/Kl$, the trajectory ‘‘amplitude’’ $A_H = \tanh(\frac{1}{2}\Delta z/L_H)$ determined by the initial separation from equilibrium $\Delta z = z(0) - z_E$ at time $t = 0$, and the characteristic hop time

$$T_H = T_D \left(\frac{L_H}{l} \right) \frac{2\pi}{\sqrt{|\Phi^2 - 1|}} \exp \left(\frac{\Delta U}{k_B T} + \frac{1}{4} \frac{l}{L_H} \right). \quad (8)$$

In Eq. 8 we introduced the ratio $\Phi = \frac{1}{2}\Delta U\lambda^2/K$ between the free energy curvature of the modeled perturbation and that of a smooth spherical particle. The characteristic hop length, L_H , and time, T_H , in our model are thus determined by two independent parameters, (i) the dimensionless energy barrier $\Delta U/k_B T$ and (ii) the dimensionless wavelength $l/\sqrt{k_B T/\gamma}$, while the dynamics of relaxation also depends on the dimensionless initial condition $\Delta z/L_H$. Sufficiently far from equilibrium when $|z - z_E|/L_H \gg 1$, we have $\langle z \rangle = z_E + L_H \log[\frac{1}{2}t/T_H + \exp(\Delta z/L_H)]$, which is equivalent in form to the logarithmic expression recently employed in Ref. [10] to fit experimental observations by treating L_H and T_H as adjustable parameters. It is noteworthy that Eq. 7 predicts a crossover to exponential relaxation, $\langle z \rangle = z_E + \Delta z \exp(-t/T_H)$, for $|z - z_E|/L_H \ll 1$ when the particle is very close to equilibrium.

To verify our analytical predictions, derived under the assumption of a quasi-static process and (overdamped) Brownian motion [13, 14], we perform numerical simulations via standard MD techniques [18]. The simulated system, illustrated in Fig. 1(c), has three atomic species: ($i=1$) fluid 1; ($i=2$) fluid 2; ($i=3$) the solid particle and bottom wall. As in previous work [19], our MD simulations employ generalized Lennard-Jones potentials $V(r) = 4\epsilon[(r/\sigma)^{-12} - c_{ij}(r/\sigma)^{-6}]$, where ϵ is the interaction energy, σ roughly corresponds to the atomic diameter, r is the distance between any two atoms, and $c_{ij} = c_{ji}$ is the interaction coefficient between species ($i, j = 1-3$). In this work we set $c_{ii} = 1$ for self interactions, while in the case of cross interactions we set $c_{12} = 0.5$ for the fluids, $c_{13} = c_{23} = 0.35$ for the fluids and Brownian particle, and $c_{13} = c_{23} = 0.8$ for the fluids and stationary bottom wall. At a simulated constant temperature

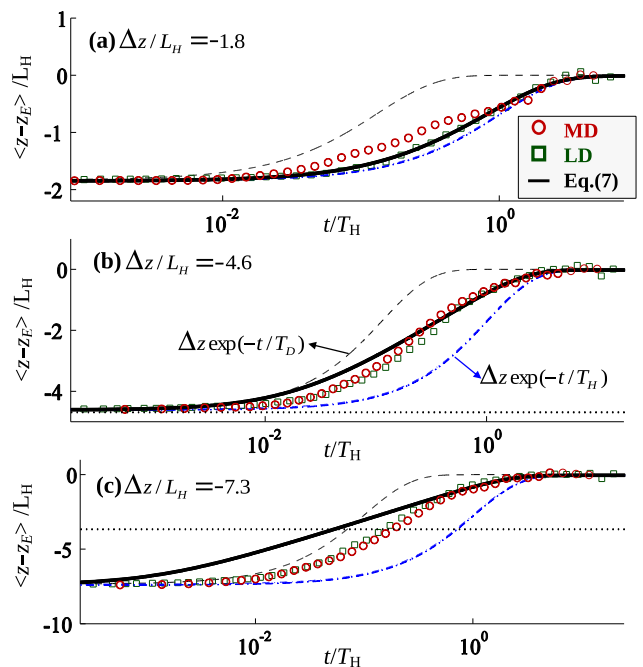


FIG. 2. Mean trajectories $\langle z(t) - z_E \rangle$ and relaxation regimes. Horizontal dotted lines indicate the distance from equilibrium $\Delta z_H = \frac{1}{2}\pi\Delta U/Kl$ above which hopping dominates. Markers indicate numerical simulations via MD and LD (see legend). Solid lines indicate analytical predictions from Eq. 7. Dashed lines indicate exponential relaxations at the viscous decay time $T_D = \xi/K$ and the hop time T_H from Eq. 8 (see labels). The energy barrier is $\Delta U = 4k_B T$, and the perturbation wavelength is $l = 4.5\sqrt{k_B T/\gamma}$ for all three initial conditions: (a) $\Delta z/L_H = -1.8$; (b) $\Delta z/L_H = -4.6$; and (c) $\Delta z/L_H = -7.3$.

$T = 3\epsilon/k_B$, maintained by a Nosé-Hoover thermostat, and a number density $\rho = 0.8/\sigma^3$, the fluids are macroscopically immiscible and the surface tension measured across a plane interface [20] is $\gamma \simeq 1.4k_B T/\sigma^2$. Solid surfaces exhibit neutral wetting ($\theta_E = 90^\circ$) given the symmetry of fluid-solid interactions. All fluid and solid atoms have a unit mass and are initialized on a fcc lattice (cf. Fig. 1(c)) with spatial spacing $\Delta x = \sqrt[3]{1/\rho}$. The solid particle and wall, carved from the fcc lattice, thus are neutrally buoyant. The particle has length $L_T = 40\Delta x$ and a nearly sinusoidal roughness (cf. Fig. 2(c)) with wavelength $l = 6\Delta x$, height $h = 2\Delta x$, and width $w = 2h$ that we expect to produce the free energy perturbation modeled in Eq. 3. In different numerical realizations, fluid atoms are initialized with random velocities and the particle is allowed to move in the vertical z direction after thermal equilibrium is attained. The hop length $L_H = 2k_B T/Kl$ in MD simulations is modified by adjusting the ‘‘spring’’ stiffness K . In addition, we perform Langevin dynamics (LD) simulations which are equivalent to numerical solution of Eq. 1.

Ensemble-averaged trajectories $\langle z(t) \rangle$ are reported in

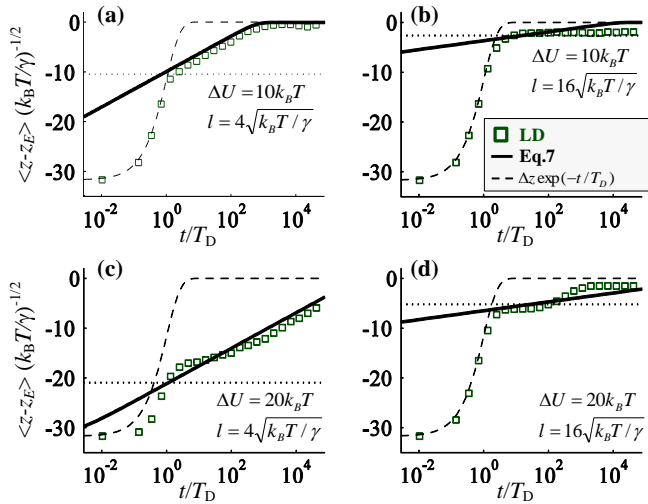


FIG. 3. Crossover from exponential to logarithmic relaxation. Solid lines indicate logarithmic relaxation given by Eq. 7. Dashed lines correspond to an exponential decay at rate $1/T_D$. Dotted horizontal lines show the distance to equilibrium $\Delta z_H = \frac{1}{2}\pi\Delta U/Kl$ near which the crossover occurs.

Fig. 2 for three different displacement amplitudes $|\Delta z| = |z(0) - z_E| \simeq 2-7L_H$. The simulated case corresponds to an energy barrier $\Delta U = 4k_B T$ and a perturbation wavelength $l = 4.5\sqrt{k_B T/\gamma}$. Very close to equilibrium for $|\Delta z|/L_H < 2$ (cf. Fig. 2(a)), the relaxation is exponential at the slower rate $1/T_H$ predicted by Eqs. 7-8. Far from equilibrium (cf. Figs. 2(b-c)) where $|z - z_E| > \Delta z_H = \frac{1}{2}\pi\Delta U/l$, the relaxation is exponential at the “fast” rate $1/T_D$ predicted by Eqs. 1-2 for a stable system; T_D is numerically computed using large values of K for which there is no metastability. Closer to equilibrium where $|z - z_E| < \Delta z_H$, numerical results are in close agreement with Eq. 7 valid for quasi-static transitions between metastable states.

Additional simulations for larger energy barriers $\Delta U = 10-20k_B T$, different perturbation wavelengths $l = 4-16\sqrt{k_B T/\gamma}$, and a larger separation from equilibrium $|\Delta z| = 32\sqrt{k_B T/\gamma} = 20-82L_H$ are reported in Fig. 3. The resulting relaxation times T_H in the logarithmic regime are extremely long and these simulations were only feasible via LD. At a distance $\Delta z_H = \frac{1}{2}\pi\Delta U/Kl$ we observe the crossover from a fast exponential relaxation, dominated by free energy minimization, to a slow logarithmic relaxation predicted by Eq. 7, dominated by the thermally-activated escape from metastable states. The crossover to a slow logarithmic relaxation is delayed, or even prevented, when increasing the wavelength l of the perturbation, cf. Figs 3(a-b), or decreasing the energy barrier ΔU , cf. Fig. 3(a) and Fig. 3(c).

It is useful to examine how features of the energy perturbations and physical properties of the media determine the relaxation time T_H in the logarithmic regime.

According to Eq. 8 the dimensionless hop time, $T_H/T_D = f(\Delta U/k_B T, l/\sqrt{k_B T/\gamma})$ is a function of the dimensionless amplitude and wavelength of the energy perturbation. Given the functional form of Eq. 8, it is convenient to analyze the function $\log(T_H/T_D) = P - Q$, where $P = \Delta U/k_B T + \frac{\pi}{4}\gamma l^2/k_B T$ is the dominant contribution. One finds that not only increasing the energy barrier ΔU , but also increasing the wavelength l causes an exponential increase in the relaxation time T_H . Extremely large relaxation times T_H produced by large perturbation wavelengths $l > \sqrt{k_B T/\gamma}$, indicate that the particle will be jammed, i.e., prevented from reaching equilibrium, as soon as the hopping motion begins. However, when the wavelength l of the heterogeneity is large the particle can get much closer to equilibrium before jamming because the hopping motion begins at a much later stage when $|z - z_E| \simeq \Delta z_H \sim \Delta U/Kl$. Therefore, a logarithmic relaxation on experimentally accessible time scales can be observed provided that the energy perturbation wavelength $l < \sqrt{k_B T/\gamma}$ is smaller than the root-mean-square displacement of the fluid interface.

In order to discuss our findings let us consider a physical system of practical importance, a one-micron radius and nearly spherical particle adsorbed at a water-oil interface for which $\gamma = 0.04\text{N/m}$ and $k_B T = 4 \times 10^{-21}\text{J}$ at room temperature. The contact line perimeter is then $p \simeq 6 \times 10^{-6}\text{m}$. We further consider an energy barrier $\Delta U = \gamma\Delta A = 30k_B T$, much smaller than the microparticle adsorption energy, caused by a surface feature of area $\Delta A \simeq 3\text{nm}^2$. If the feature is well localized only a small portion of the contact line hops over the feature while most of its perimeter remains pinned. Hopping over localized features, the contact line moves in steps of average length $\Delta A/p \simeq 0.5 \times 10^{-12}\text{m}$. This distance corresponds to an energy perturbation wavelength $l \simeq 0.002\sqrt{k_B T/\gamma}$ which results in a relaxation time $T_H \simeq 10^3\text{s}$. The logarithmic regime will then begin at $|z - z_E| \lesssim 5 \times 10^{-7}\text{m}$, i.e., half a radius away from the expected equilibrium. This scenario corresponds to experimental conditions in Ref. [10]. Moreover, using a wavelength $l \simeq 0.5-1 \times 10^{-12}\text{m}$ and energy barriers $\Delta U \simeq 15-30k_B T$, we find that Eq. 7 fits closely experimental data in Ref. [10] that were qualitatively reproduced via a different approach (See [21, 22] for a detailed discussion).

In conclusion, we have derived analytical expressions for colloidal adsorption via Kramers’ escape rate from metastable states. We found that certain sizes and wavelengths of localized heterogeneities can give rise to physical aging and jamming (ultimately observed as static contact angle hysteresis). Our analysis and numerical simulations document a crossover from a fast exponential relaxation to slow logarithmic/exponential relaxations, at a distance $|z - z_E| \sim \Delta U/\gamma l$ from the expected equilibrium. These results demonstrate a nontrivial adsorption dynamics that is prescribed by the microscale geometry of the particle surface.

We are thankful to Prof. Vinothan N. Manoharan and Ms. Anna Wang for helpful discussions. This work was supported by the NSF PREM (DMR-0934206).

* ccolosqui@ccny.cuny.edu

† Department of Chemical Engineering, City College of the City University of New York, New York, NY 10031, USA; morris@ccny.cuny.edu

‡ Physics Department, City College of the City University of New York, New York, NY 10031, USA; koplik@sci.ccny.cuny.edu

- [1] P. Kralchevsky and K. Nagayama, *Particles at Fluids Interfaces and Membranes*, Vol. 10 (Elsevier Science, 2001).
- [2] O. Velev and S. Gupta, *Adv. Mater.* **21**, 1897 (2009); H. Goesmann and C. Feldmann, *Angew. Chem. Int. Ed.* **49**, 1362 (2010).
- [3] R. Mezzenga, P. Schurtenberger, A. Burbidge, and M. Michel, *Nat. Mater.* **4**, 729 (2005).
- [4] A. Dinsmore, M. Hsu, M. Nikolaidis, M. Marquez, A. Bausch, and D. Weitz, *Science* **298**, 1006 (2002); K. Velikov and E. Pelan, *Soft Matter* **4**, 1964 (2008).
- [5] P. Pieranski, *Phys. Rev. Lett.* **45**, 569 (1980).
- [6] J. Israelachvili and M. Gee, *Langmuir* **5**, 288 (1989); E. Bormashenko, *Colloid Polym. Sci.*, **1** (2012).
- [7] V. Paunov, *Langmuir* **19**, 7970 (2003); L. Arnaudov, O. Cayre, M. Stuart, S. Stoyanov, and V. Paunov, *Phys. Chem. Chem. Phys.* **12**, 328 (2009).
- [8] A. Stocco, E. Rio, B. Binks, and D. Langevin, *Soft Matter* **7**, 1260 (2011).
- [9] K. Du, E. Glogowski, T. Emrick, T. Russell, and A. Dinsmore, *Langmuir* **26**, 12518 (2010).
- [10] D. Kaz, R. McGorty, M. Mani, M. Brenner, and V. Manoharan, *Nat. Mater.* **11**, 138 (2012).
- [11] T. Blake and J. Haynes, *J. Colloid Interface Sci.* **30**, 421 (1969).
- [12] L. C. E. Strum, *Polym. Eng. Sci.* **17**, 165 (1977).
- [13] H. Kramers, *Physica* **7**, 284 (1940).
- [14] P. Hanggi, *Journal of Statistical Physics* **42**, 105 (1986).
- [15] R. Aveyard and J. Clint, *Faraday Trans.* **92**, 85 (1996).
- [16] A. Marmur, *Colloid. Surface. A* **136**, 81 (1998).
- [17] MD simulations required extremely long runs (i.e., over 10 million timesteps) and several (7–10) independent realizations; running in parallel (7 CPUs at 2.20GHz) the simulations required over 300 hours of CPU time.
- [18] D. Rapaport, *The art of molecular dynamics simulation*, 2nd ed. (Cambridge University, New York, 1995).
- [19] J. Koplik and J. R. Banavar, *Phys. Rev. Lett.* **96**, 044505 (2006); G. Drazer, J. Koplik, A. Acrivos, and B. Khusid, *ibid.* **89**, 244501 (2002).
- [20] J. Koplik and J. Banavar, *Annu. Rev. Fluid Mech.* **27**, 257 (1995).
- [21] T. Blake and J. De Coninck, *Eur. Phys. J. Spec. Top.* **197**, 249 (2011).
- [22] See Supplemental Material at for a detailed discussion on fundamental differences between the model proposed in this work and that employed in [10].